EXPERIMENTAL RESPONSE OF A LOW-YIELDING, SELF-CENTERING, ROCKING COLUMN BASE JOINT WITH FRICTION DAMPERS

Massimo Latour[a], Gianvittorio Rizzano[a], Aldina Santiago[b], Luis Simoes da Silva[b]
[a]University of Salerno, Dept. Civil Engineering, Italy
[b]University of Coimbra, ISISE, Portugal

mlatour@unisa.it, grizzano@unisa.it, aldina@dec.uc.pt, luisss@dec.uc.pt

ABSTRACT

The sliding hinge joint (SHJ) is a type of supplemental energy dissipation system for column bases or beam-to-column connections of steel Moment Resisting Frames (MRFs). It is based on the application of symmetric/asymmetric friction dampers in joints to develop a dissipative mechanism alternative to the column/beam yielding. This typology was initially proposed in New Zealand and, more recently, is starting to be tested and applied also in Europe. While on the one hand this technology provides great benefits such as the damage avoidance, on the other hand, due to the high unloading stiffness of the dampers in tension or compression, its cyclic response is typically characterized by a limited self-centering capacity.
To address this shortcoming, the objective of the work herein presented is to examine the possibility to add to these connections also a self-centering capacity proposing new layouts based on a combination of friction devices (providing energy dissipation capacity), pre-loaded threaded bars and disk springs (introducing in the joint restoring forces).
In this paper, as a part of an ongoing wider experimental activity regarding the behaviour of self-centering connections, the attention is focused on the problem of achieving the self-centering of the column bases of MRFs by studying a detail consisting in a column-splice equipped with friction dampers and threaded bars with Belleville disk springs, located above a traditional full-strength column base joint. The main benefits obtained with the proposed layout are that: i) the self-centering capability is obtained with elements (threaded bars and Belleville springs) which have a size comparable to the overall size of the column-splice cover plates; ii) all the re-centering elements are moved far from the concrete foundation avoiding any interaction with the footing. The work reports the main results of an experimental investigation and the analysis of a MRF equipped with the proposed column base joints.

Keywords: Friction dampers, self-centering, FREEDAM, base-plate, modelling

** Corresponding author*

1. INTRODUCTION

Eurocodes require to design structures to ensure the achievement of minimum performance levels under a set of design load combinations [1,2]. Current design procedures are based on structural checks for Serviceability Limit States (SLS) (related to the most frequent conditions occurring during the life-time of the structure) and for Ultimate Limit States (ULS) for which the structure, in case of rare seismic events, can be designed to dissipate energy in selected zones.

The modern seismic protection strategies implemented into international building codes are based, in case of destructive seismic events, on the absorption of the seismic energy in dissipative zones, which are detailed to sustain cyclic inelastic rotation demands [3]. In case of steel Moment Resisting Frames (MRFs) this strategy is traditionally applied by properly over-strengthening columns and connections enforcing, in this manner, the development of plastic hinges in the beam ends and at the base of the columns. Additionally, to maximize the energy dissipation, the plastic zones are spread along the elevation of the building, promoting the development of a global failure mode through the application of members hierarchy criteria and the design of full strength connections [4-7]. Therefore, owing to the assumptions made in design, traditional procedures typically lead to structures characterized by weak beams and column bases, with strong joints.

This approach, if on the one hand provides benefits, such as the development of a stable plasticization and the reduction of the inter-storey drifts under serviceability loading conditions, on the other hand, leads to significant shortcomings. The most substantial weakness is intrinsic in the design strategy itself. In fact, although the damage is needed to absorb the input earthquake energy, it also represents one of the main sources of economic loss [8-11]. In fact, since the dissipative zones are constituted by sections or elements belonging to the structural system, after severe seismic events, the structure is affected by significant damage and, because of permanent plastic deformations, it is characterized by a pattern of residual drifts. In general, the magnitude of this out-of-plumbness may be significant in view of the actual possibility to repair the structure after a destructive seismic event.

Aiming to design structures undergoing minimal damage, special typologies of dissipative partial strength joints based on the inclusion of friction dampers in connections have been proposed and, recently, extensive studies have been carried out in research programs

worldwide [12-15]. These connections were initially proposed by Grigorian and co-authors in 1993 [16] and, subsequently, many other theoretical, experimental and modelling works, as well as practical applications, were carried out, especially in New Zealand, developing the so-called called Sliding Hinge Joint (SHJ). This connection is characterised by very simple details based on the inclusion of Asymmetric Friction Connections (AFC) or Symmetric Friction Connections (SFC) at the bottom beam flange, with friction pads made of mild steel, aluminium, brass or – in the most recent versions – abrasion-resistant steel (e.g. [16-22]). Similar solutions were also patented in 2000 in Japan [23,24] while, more recently, other alternatives have been proposed suggesting new layouts, in which the friction damper is conceived as a separate element fabricated in the shop and fastened on site to the beam bottom flange [25-28]. This layout, which is probably not as simple as the SHJ, provides the possibility to realise the whole damper in the shop allowing a better control on the materials quality (e.g. higher control of the surface conditions, continuous factory controls on the production, control on the employed bolts quality), and on the application of rigorous bolts installation procedures complying with the relevant European standards [28-34]. The layout of the typical beam-to-column joint, recently proposed in Europe for application in semi-continuous steel Moment Resisting Frames (MRFs), represents an alternative to a stiffened Double Split Tee connection (DST) where, in place of the bottom Tee, a slotted friction device with a haunch slipping on friction shims pre-stressed with pre-loadable high strength bolts (Fig.1) is realised. All the elements of the connection constitute a Symmetrical Friction Connection (SFC) which is, as already underlined, a friction damping device fabricated as a standalone element in the shop. With such detail the beam is forced to rotate around the pin located at the base of the upper T-stub web and the energy dissipation is ensured by the alternate slippage of the lower beam flange on friction shims (Fig.1).

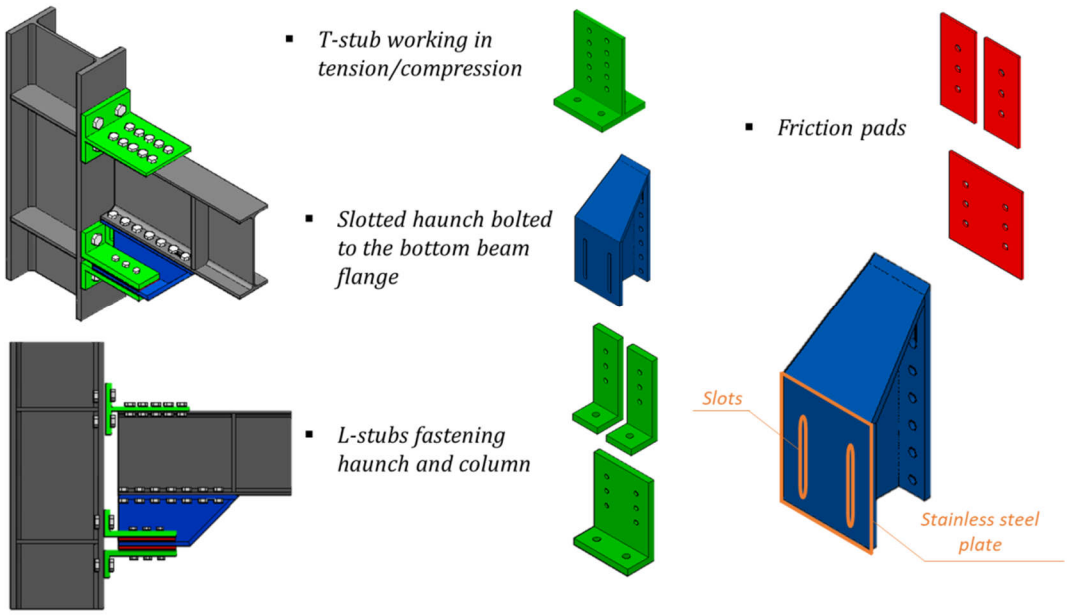

Fig. 1 **–** Typical layout of one of the connections studied in [28]

This connection, similarly to the SHJ, should be implemented to behave rigidly at SLSs and to allow the beam-to-column inelastic rotation at the ULS. Additionally, through the application of proper hierarchy criteria, both at the global and local level, it can be easily designed to be the only source of energy dissipation of the whole structure.

Within this framework, considering the encouraging outcomes of previous research projects dealing with the application of such connections, in this paper, the problem of the self-centering structures equipped with dissipative friction joints is analysed. In fact, due to permanent deformations in the friction dampers, similarly to what occurs when plastic zones are concentrated in the beams or in yielding connections, significant out-of-plumbness displacements can remain after a severe ground motion [15, 42-44]. Indeed, although these connections are very effective from the point of view of the damage avoidance, they still provide significant problems related to the low self-centering capacity. This drawback is mainly due to the high unloading stiffness of the friction dampers in tension or compression. To avoid this undesired behaviour, as already proposed in several past studies [34-41] a supplemental re-centering system can be adopted.

Specifically, in this paper, the attention is focused on the problem of self-centering the column base joint, by studying a detail consisting in a column-splice equipped with friction dampers and threaded bars with Belleville disk springs, located just above a traditional full-strength base plate joint. The main advantages of the proposed layout are that: *i)* the self-centering capability is obtained with re-centering elements (threaded bars and Belleville springs) which

have a small size, similar to the dimension of the column-splice cover plates; *ii)* all the re-centering elements are moved far from the concrete foundation. The work reports the main results of an experimental investigation and preliminary analyses of MRFs equipped with re-centering FREEDAM column base joints. The obtained results are hereinafter critically discussed showing the promising performances of the proposed column base connection.

2. CONCEPT OF THE PROPOSED CONNECTION

2.1 Friction dampers and re-centering systems

Being an effective way of dissipating energy, dampers based on principles of dry friction have become very popular and are largely used in high risk seismic zones. In the last decades, the application of this concept has been subject of numerous studies [35-38, 45] and many friction dampers have been proposed for practical purposes. This damper typology usually dissipates energy through the alternate slippage of at least two surfaces in contact, on which a transversal clamping force is applied with hydraulic systems [46], electromagnetic forces [47] or, in the simplest case, by means of mechanical devices such as high strength bolts. This last clamping method is the most common in civil engineering practice.

The cyclic behaviour of friction dampers is normally characterized by a rigid-plastic hysteresis which depends only on two parameters: the clamping force and the friction coefficient of the interfaces in contact. The first parameter is usually governed by the application tightening procedures which are based essentially on the control of the nut rotation (displacement-controlled procedure), applied torque (force-controlled procedure) or on the employment of specific devices which fail or squash at the achievement of the proof preloading level (e.g. DTI or squirter DTI washers and HRC bolts) [26]. Conversely, the second parameter (namely the friction coefficient) is predicted by means of physical modelling or experimental testing. In the former case, the attention is focused on the modelling of complex and microscopic phenomena such as adhesion and ploughing which are dependent upon the surfaces topography, the materials hardness, the mechanical properties and the effects of interface layers. In the latter case, which is the most common in structural engineering practice, conversely, the properties of the friction interface are studied by means of experimental testing which, for seismic engineering purposes is generally considered sufficient to provide the information needed for designing the devices. A general discussion dealing with the main factors influencing the friction interaction is reported in [10,48,49].

147 The main proposals of application of friction dampers in steel structures are referred to
148 bracing systems or beam-to-column connections. One of the first devices based on friction
149 was that developed in [50] which introduced at the intersection of braces, brake lining pads
150 between the steel sliding surfaces. One of the simplest forms of friction damper has been
151 proposed in [51] who adopted simple bolted slotted plates located at the end of a
152 conventional bracing member. The brace-to-frame connection was designed to slip with fully
153 elastic braces. Another friction damper for chevron braces was proposed in [52]. Concerning
154 connections, as previously said, application of principles of dry friction were initially first
155 developed by Grigorian and co-authors [16] and subsequently extensive studies were carried
156 out in New Zealand by the research group at the University of Auckland [9,10, 17-22, 53,54]
157 and in other countries applying these principles also to other structural typologies [55,56].
158 More recently, other works on a specific type of sliding hinge joint have been performed also
159 in Europe in a research activity regarding the analysis of friction materials, the bolt
160 installation procedures, the long-term response due to relaxation of the slip force, the
161 robustness assessment, the FE modelling and the experimental analysis of real-scale
162 structures or sub-assemblies of joints [26,28].
163 While, as herein summarized, friction dampers in beam-to-column connections have been
164 largely investigated, the application of friction dampers in column base joints of steel
165 structures is only a recent proposal and little knowledge is currently available. The idea to
166 dissipate energy in the base plate with friction devices comes from the field observation of
167 damages after the earthquakes of Northridge (1994), Kobe (1995) and Tohuku (2011). In fact,
168 during the technical surveys, in many cases, severe damage involving plate and anchor bolts
169 was observed. Additionally, past experimental tests have indicated that the traditional base
170 plate connections are prone to the development of damage into elements which are not easy
171 to replace such as the base section of the column (in case of full-strength connections) or the
172 base plate/anchors (in case of partial strength connections) and, due to residual
173 deformations, may give rise to a pattern of residual lateral displacements in the whole
174 building. Therefore, in general, owing to the limited dissipative capacity and difficult
175 reparability of the base joint (they are typically hidden by the flooring of the first storey) the
176 occurrence of damage at the base of the building represents a significant shortcoming both in
177 view of the actual reparability of the building and in terms of economic cost to be sustained in
178 the aftermath. All these issues have recently motivated a significant number of research
179 activities worldwide dealing with the development of innovative base plate connections

equipped with dampers able to limit damage, while preserving the ability of the structure to dissipate energy in case of rare seismic events. These connections, in some cases, have been equipped also with re-centering elements able to restore the columns to the initial position.

Two layouts were proposed by McRae and co-authors [58], while in [59] the study of the efficiency of the dissipation of seismic energy through column base solutions has been performed carrying out a series of experimental tests on different low damage steel base connection. Within this work, two new design solutions were tested: the weak axis aligned asymmetric friction connection, where friction surfaces are parallel to the web on plates outstanding from the column flange, the strong axis aligned asymmetric friction connection, where friction surfaces are parallel to the column flange. It is worth noting that, as evidenced in [58], critical phenomena occurring with conventional full-strength connections can be mitigated by means of friction column base connection, such as that proposed in this paper. In fact, while in traditional frames due to yielding of the column base section and local buckling phenomena, axial shortening of the column may occur [58, 60], with damage free connections, such as the double friction base columns suggested in [58, 59] owing to the absence of plastic deformations in the column, the axial shortening and its detrimental effects can be completely avoided. Recently a novel type of rocking damage free connection has been proposed in [15]. This column base, has a circular hollow section welded to a thick plate, four post-tensioning tendons to give a self-centering capacity to the connection and friction dampers to dissipate energy.

Other practical cases of self-centering systems proposed in literature usually include a tendon, applied in the joint or over the entire extension of the structure. In [39] it was proposed to include friction ring springs to the SHJ, obtaining a flag-shape behavior of the connection. A similar approach in terms of re-centering was proposed in [40] who employed as re-centering component rods applied at the tips of the whole beam, rather than only on the joint. In this work, the introduction of an “active link” was suggested and the connection to the beam, at both ends, was achieved by means of pre-tensioned rods. In the second work, the employment of a set of rods going through the entire segment of the beam and attached in the joint section was proposed.

Self-centering base connections have also been developed in [41] using post-tensioned rods anchored to the column foundation. The aim is to ensure the possibility of movement, pre-stressing the rods within their elastic capacity. However, the proposed solutions, based on anchoring the rods to the foundation, can be less effective in a replacement situation. Friction

systems can also show a self-centering ability when employed with an asymmetric configuration of the damper [21]. However, such capability is usually limited, and additional components are normally needed to restore the connection itself or the structure. A significant practical implementation of the damage avoidance design strategy is described in [57]. In this project, the building is designed in the transverse direction with tension limited rocking shear walls and in the opposite direction with Sliding Hinge Joint MRFs. In this application, the rocking shear walls are equipped with Ringfederer springs to obtain the self-centering ensuring hinge formation under a stable rocking mechanism. Conversely, the MRF bays are equipped with conventional SHJs without self-centering devices. The similarities between the solutions adopted in [57] and the application described in this paper are related to the adoption of heavy-load springs to adjust the capacity of the structure and the introduction of friction dampers in the column base. Nevertheless, as a difference, the connection hereinafter presented proposes to introduce in the column base a simple system of threaded bars with sets of Belleville washers acting as a spring to provide the needed self-centering action. This proposal wants to keep the layout of the connection as simple as possible providing, other than the self-centering capacity, additional benefits such as the absence of interaction with the concrete foundation and the limited size of the connection which is, overall, similar or lower than the size of the cover plates employed to realize a traditional column splice connection.

2.2 Proposed Solution

The proposed connection consists in a slotted column splice equipped with friction pads located above a traditional full-strength base plate joint (Fig. 2a) [38]. In particular, symmetrical friction dampers are realized slotting the upper part of the column above the splice, adding cover plates and friction pads pre-stressed with high strength pre-loadable bolts on both web and flanges. To allow the gap opening, the slotted holes are designed to accommodate a minimum rotation of 40 mrad [60], which is the benchmark rotation established by AISC 341-16 for Special Moment Frames (SMFs). Similar provisions are given in EC8 [3], which requires for Ductility Class High frames a rotation of 35 mrad. Between the steel plates and the column, friction pads are inserted. It is worth noting that the layout presented in this paper is not explicitly considering the possibility to accommodate a similar rotation also in the weak direction, which is, instead, a situation rather common in practice. Nevertheless, to provide a biaxial rotation capacity to the connection it would be sufficient to

246 oversize slightly the flange slots following the same simple geometrical rules used to over-size
247 the web holes.

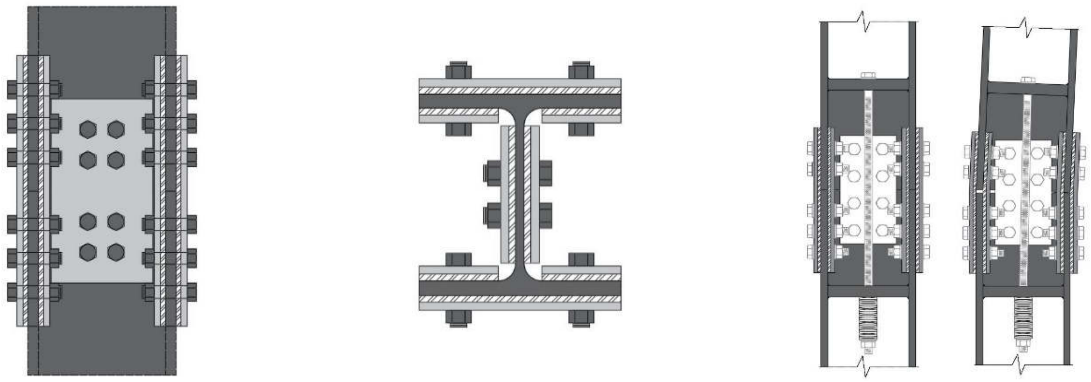

a) Friction connections b) Re-centering system

Fig. 2. Concept of the proposed solution

248

249 To provide a self-centering capability, pre-loaded threaded bars are introduced (Fig. 2b).
250 Additionally, to provide a sufficient deformability to the bar, a system of disk springs arranged
251 in series and parallel is installed in the assembly.
252 To assess the overall response of the connection (sub-assembly of Fig. 3a), the behavior of the
253 whole system (connection, flange and web friction pads, re-centering bars and column) can be
254 idealized by means of the simplified mechanical model delivered in Fig. 3b. The rotational
255 spring C_b accounts for the flexural stiffness of the cantilever column of length equal to l_0 (Fig.
256 3a), given by:
257

$$K_{Cb} = \frac{3E_s I_c}{{l_0}^3} \tag{1}$$

258 where E_s is the steel modulus of elasticity, l_0 is the column length up to the splice section and I_c
259 is the moment of inertia of the column profile. The translational spring F_f models the friction
260 pads on the column flanges.

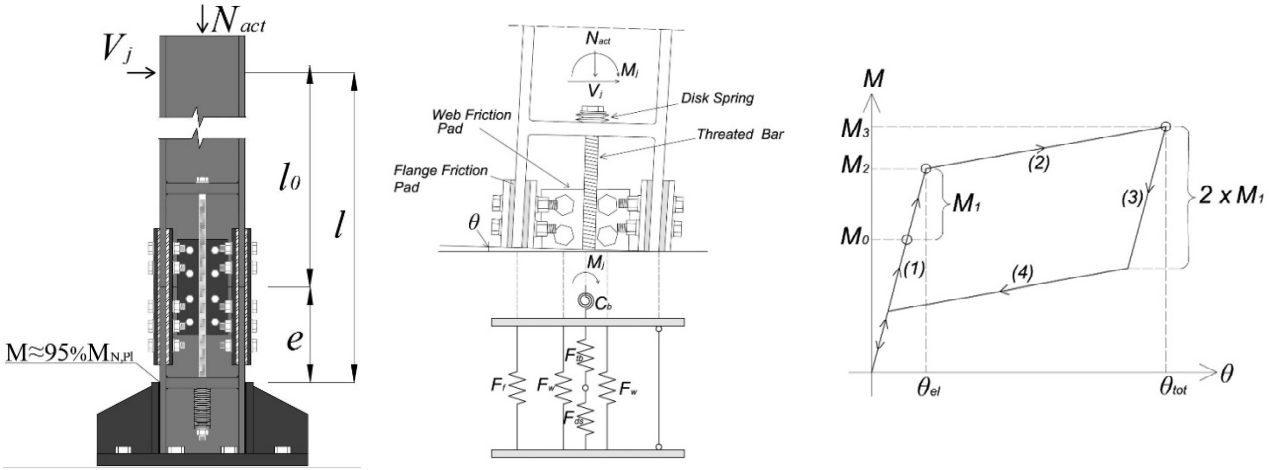

a) Joint subassembly

b) Connection mechanical model

c) Theoretical moment-rotation relationship

Fig. 3. Concept of the proposed solution

The stiffness of this component can be assumed infinite up to the achievement of the slip force and equal to zero when this value is achieved. Similarly, F_w models the friction pads on the column web. The translational spring F_{tb} models the axial behaviour of the threaded bars which work in series with the system of disk springs, whose resistance is defined as F_{ds}. The stiffness of the threaded bars is given by:

$$K_{tb} = \frac{n_b E_{tb} A_{tb}}{l_{tb}} \tag{2}$$

and the stiffness of the disk springs is expressed as:

$$K_{ds} = \frac{n_b n_{par}}{n_{ser}} K_{ds1} \tag{3}$$

where n_b is the number of bars employed in the connection symmetrically with respect to the centroid of the column, n_{par} is the number of disk springs in parallel, n_{ser} is the number of disk springs in series and K_{ds1} is the stiffness of the single disk spring. Considering this mechanical model, it is easy to verify that the typical moment-rotation behaviour of the connection can be represented by a flag shape (Fig.3c). The moment M_2 represents the decompression moment which corresponds to attainment of the slippage force in all the friction pads. The first branch of the moment-rotation curve is characterized by an infinite stiffness of the connection and, therefore, the rotational stiffness of the whole system is equal to K_{Cb}. The second branch,

corresponds to the gap opening. In this phase, the slippage of the friction pads occurs, and the rotational stiffness of the system is due to the stiffness of the threaded bars, disk springs and column in bending, namely:

$$K_2 = \frac{1}{\frac{1}{K_{Cb}} + \frac{4}{h_c^2}\left(\frac{1}{K_{tb}} + \frac{1}{K_{ds}}\right)} \tag{4}$$

where h_c is the column height. The branches 3 and 4 are characterized by the same stiffness of the branches 1 and 2, respectively. The bending moment M_0 represents the decompression moment due to the sum of the axial load in the column and to the pre-stress of the threaded bars:

$$M_0 = (F_{tb} + N_C)\frac{h_c}{2} \tag{5}$$

The bending moment M_1 represents the contribution to the bending moment due to friction pads, equal to:

$$M_1 = F_f\left(h_c - \frac{t_{fc}}{2}\right) + F_w\frac{h_c}{2} \tag{6}$$

where t_{fc} is the thickness of the column flange. Considering these equations, it is easy to verify that, from design point of view, the re-centering of the connection can be guaranteed imposing that:

$$M_0 - M_1 \geq 0 \quad \Rightarrow \quad F_{tb} \geq F_f\left(2 - \frac{t_{fc}}{h_c}\right) + F_w - N_c \tag{7}$$

3. DESIGN OF THE SPECIMENS FOR EXPERIMENTAL TESTS

With the set of equation previously reported, starting from the definition of the design actions, a column base connection has been designed. Owing to reasons of compatibility of the specimen capacity with the available equipment, the axial load has been limited to the 25% of the squash load, while the bending moment acting in the splice has been set equal to the 95% of the plastic bending moment of the column. The shear load derives from the testing scheme which is a cantilever representing, approximately, half column of the first storey of the

building. Therefore, starting from a column profile HEB240, steel class S275, the following design values have been calculated:

$$N_d = \nu\, N_{pl} = 0{,}25\, N_{pl} = \ 728{,}75\ kN \quad (8)$$

$$M_d = 198{,}5\ kNm \quad (9)$$

$$V_d = \frac{M_j}{l_0} = 128{,}1\ kN \quad (10)$$

where l_0=1,55 m is the distance between the force at the top of the column and the splice (Fig.3a), N_{pl} is the column squash load, ν is the axial load ratio, M_d is the assumed design bending moment for the column base connection and V_d is the design value of the shear force. Based on the shear design load V_d, firstly, the web component has been designed imposing that the slippage force on the web has to resist the applied shear load. All plates are of S275 steel class. The friction pads have been chosen according to the results of previous tests on friction materials [62]. Basing on these results a friction coefficient μ=0,6, has been assumed. Considering four bolts for both the upper and lower sides of the web connection, the pre-load F_{wp}, for each bolt, has been determined as:

$$V_d = F_w = \mu\, F_{wp}\, n_b\, n_s \quad \Rightarrow \quad F_{wp} = 26{,}7\ \ kN \quad (11)$$

where F_w is the slip resistance of the web friction dampers, μ is the design value of the friction coefficient, F_{wp} is the preloading force of the web bolts, n_b is the number of web bolts and n_s is the number of friction interfaces (in this case, considering the symmetrical configuration, this is equal to two). Considering the design resistance, M14 HV bolts of 10.9 class have been selected (HV stands for “Hochfeste Bolzen mit Vorspannung”, which in English means “high resistance bolts for pretension”). In order to design the re-centering threaded bars, according to Eq. (7), it has to be considered that the force in the bars depends on the slippage force of the flange friction pads. Therefore, imposing the global equilibrium between the internal and external bending moment in correspondence of the splice, the following system can be

written to design F_{tb} (the preloading force of the threaded bar) and F_f (the slip resistance of the flange dampers)

$$\begin{cases} F_{tb} - F_f\left(2 - \frac{t_{fc}}{h_c}\right) \geq F_w - N_d \\ F_{tb}\ \frac{h_c}{2} + F_f\ \left(h_c - \frac{t_{fc}}{2}\right) = M_d - (F_w + N_c)\ \frac{h_c}{2} \end{cases} \quad (12)$$

where h_c is the column depth and t_{fc} is the column flange thickness. For the sake of simplicity, if the lever arm of the friction force of the column flange friction dampers is approximated with h_c, the system of equations (12) leads to the following simple design formulation:

$$F_{tb} \geq \frac{M_d}{h_c} - N_d \quad \Rightarrow \quad F_{tb} \geq 98{,}6\ kN \quad (13)$$

Considering the design actions, for the specimens, two M20 threaded bars, having a maximum capacity of 171,5 kN of pre-loading, have been adopted for the re-centering system. Considering this capacity, the bar preload has been fixed equal to 100 kN. Therefore, system (12), provides the following value of the design slippage force of the column flange friction pads:

$$F_f = \frac{M_d}{h_c} - \frac{1}{2}\ (F_w + N_d + F_{tb}) \quad \Rightarrow \quad F_f = 298{,}9\ kN \quad (14)$$

Considering four bolts for both the upper and lower sides of the column flange connection, the necessary pre-load F_{fp}, for each bolt, is:

$$F_f = \mu\ F_{fp}\ n_b\ n_s \quad \Rightarrow \quad F_{fp} = 62{,}3\ kN \quad (15)$$

In this case, M20 HV bolts of 10.9 class have been selected. The last step of the design procedure consists in the design of the disk springs. Assuming a maximum rotation for the joint equal to 40$mrad$, the maximum gap-opening at the level of the re-centering bar is 4,8mm (0.04x120 mm). Adopting standard disk springs with diameter equal to 45 mm, thickness equal to 5 mm and height of the internal cone equal to 1.4 mm, three disk springs in parallel

are necessary to resist to the bar yielding force. The resistance of each disk spring is about 80 kN, while the stiffness (K_{ds1}) is about 80 kN/mm. Considering the previously defined maximum displacement, Eq. (3) provides a minimum number of 21 disk springs to be arranged in sets of 3 springs in parallel (so-called "nested" configuration), 7 times in series (so-called "back-to-back" configuration), leading to an overall stiffness equal to K_{ds}=35,36 *kN/mm*.

4. CYCLIC AND PSEUDO-DYNAMIC TESTS

The testing equipment is depicted in Fig. 4. Two actuators have been used: the first one, at the top of the column is a MOOG Actuator (Maximum Load 3000 kN) governed under load control in order to apply the axial load, the second one is an MTS 243.35 actuator, with a maximum load capacity of 385 kN in compression and 240 kN in tension and a piston stroke of 1016 mm, controlled under displacement control in order to apply a cyclic force at the top of the column.

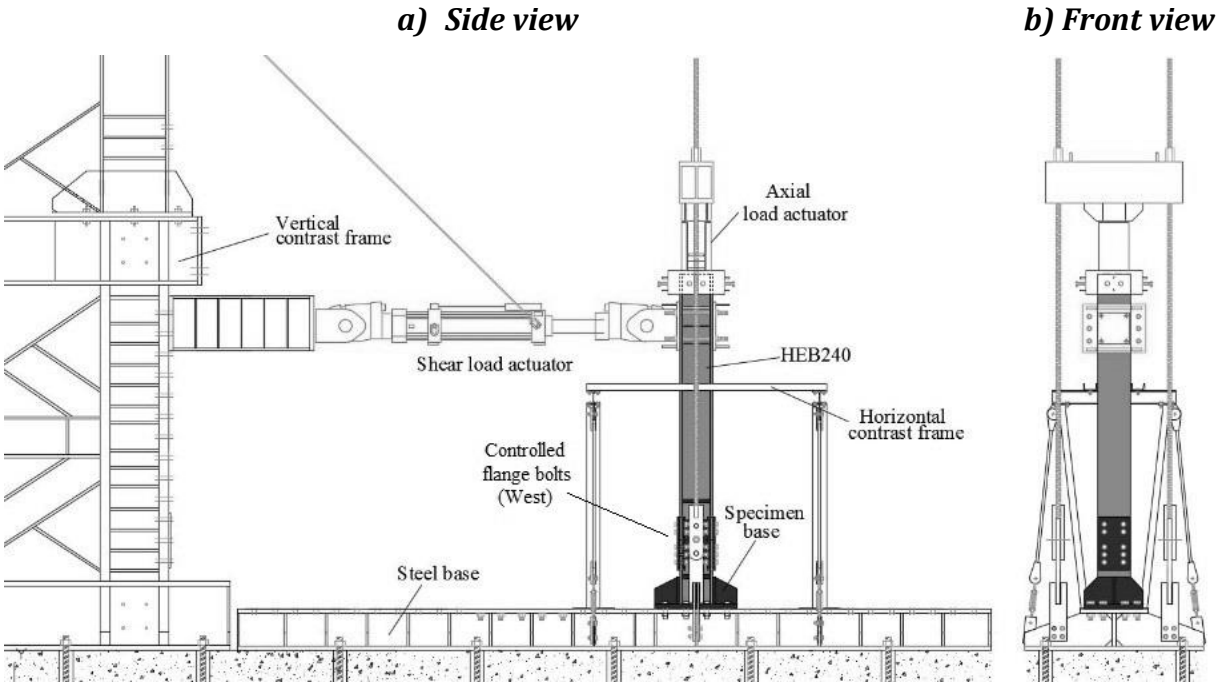

Fig. 4. Experimental layout. a) side view; b) front view

Regarding the measurement devices, a torque sensor Futek TAT430 has been used to measure the initial torque applied to the bolts with the torque wrench, while four load cells Futek LTH500 (capacity equal to 222kN) have been installed in the connection to monitor the

tensile forces in the threaded bars and in two bolts of one of the flange friction dampers (Fig. 5c). Additionally, LDT displacement transducers (max. 50mm) have been adopted in order to measure the vertical displacements in both column sides (Fig. 5c). Regarding the bolt tightening procedure the initial pre-load, according to EN 1090-2 specifications, was increased of the 10% of the preload was added to the bolt loads to account for random variability of the bolt tightening and initial installation loss. Thus, a torque of 180 Nm was applied in the flanges and 60 Nm in the webs, leading to a force of 70kN and 30kN, respectively. The pre-loading of the threaded bars was achieved by direct observation of the load cells output. Concerning the actions, the axial force was kept constant during the test, while the cyclic horizontal load at the top of the column was applied consistently with the loading protocol suggested by AISC 360-10. Four cyclic tests have been performed varying the axial load in the column, including or not including the re-centering bars.

(a) (b) (c)

Fig. 5. (a) Experimental layout; (b) Connection during the assembly; (c) view of the joint before the test

In the different tests axial load ratios equal to 25% and 12,5% have been applied. The axial loads were selected in a reasonable range of variation considering the typical size of MRFs designed according to EC8. Specific values, in general, obviously depend on the building plan and frame configuration. Nevertheless, values ranging from 10% to 30% seem representative of MRFs designed in DCH [60,63]. The adoption of a constant axial force is clearly not reproducing the real loading situation of all the columns of a moment resisting frame. In fact, due to overturning bending moments, especially the external columns of MRFs usually undergo axial force variations during the earthquake. The choice to adopt a constant axial

force was done only to simplify the equipment used, as it is normally done in literature in similar tests [64]. From the practical point of view, this situation better reproduces the behavior of internal columns which, typically, undergo lower axial load fluctuations during the seismic event. In the tests with lower values of the column axial load, the total axial load in the re-centering bars has been increased to 280 kN, which is still compatible with the pre-loading capacity of the threaded bars but not sufficient to respect Eq. (7) for guaranteeing the flag shape behavior. In Table 1, a summary of the main values related to the loading condition of the specimens is given.

Table 1. Main test data

Test Number	***Typology of Test***	***Column Axial Load*** ***kN***	***Total axial load in recentering bars*** ***kN***	***Ratio between the applied load in recentering bars and the minimum one given by Eq.(7)***	***Preloading of each web bolt*** ***kN***	***Preloading of each flange bolt*** ***kN***	***Residual rotation at the end of the test (Residual top displacement/l_0)*** ***[mrad]***
1	*Cyclic*	*728 (25% N_p)*	*200*	*2.03*	*27*	*62*	*2.1*
2	*Cyclic*	*728 (25% N_p)*	*0*	*-*	*27*	*62*	*4.1*
3	*Cyclic*	*365 (12.5% N_p)*	*280*	*0.48*	*30*	*114*	*31.0*
4	*Cyclic*	*365 (12.5% N_p)*	*0*	*-*	*30*	*114*	*49.7*
5	*Pseudo-dynamic*	*728 (25% N_p)*	*200*	*2.03*	*27*	*62*	*1.7*
6	*Pseudo-dynamic*	*728 (25% N_p)*	*0*	*-*	*27*	*62*	*5.2*
7	*Pseudo-dynamic*	*728 (25% N_p)*	*200*	*2.03*	*27*	*62*	*2.7*

In Figs. 6, the hysteretic curves of the experimental tests are reported. In particular, in Fig. 6a the experimental tests with higher axial load are depicted, while Fig. 6b show the tests with lower axial load ratio. The response of the connections reflected the expected behaviour, highlighting in the different cases, the effect of the re-centering bar. In fact, from the results presented in Figs.6, it can be clearly observed that the threaded bars have played an important role. Tests 1 and 2 were carried out with the higher value of the axial load ratio (25%), while test 3 and 4 were carried out with a reduced axial force (12.5%). In the first two tests the self-centering behavior was expected (because the size of the threaded bar was defined considering an axial load ratio equal to the 25%), while in the third and fourth test the self-centering could not be achieved because the initial tension in the bars was about half the preload needed to achieve the theoretical self-centering condition. The 3rd and 4th tests were carried out mainly to highlight the role of the re-centering threaded bar, even though in these

cases to obtain a full self-centering, as already evidenced, higher capacity re-centering systems should have been employed. The cyclic moment-rotation curve of test 1 (Fig. 6a, red line) highlights that the connection, with the axial force considered in the design phase, was able to return almost to the initial position with a very low value of the residual rotation (2.1 mrad), while in case of test 3 (Fig. 6b, red line) the residual rotation was higher (31 mrad) and well beyond the constructional drift normally accepted in the execution of steel structures (usually lower than 5 mrad, depending on the number of columns and height of the building) or the tolerance limit to be accepted accounting for the issues related to the building functionality (which can be assumed accounting for the existing literature as equal to 5 mrad as suggested in [65]). In any case, comparing Fig. 6a with Fig. 6b, the role of the re-centering bars can be clearly noticed in both cases.

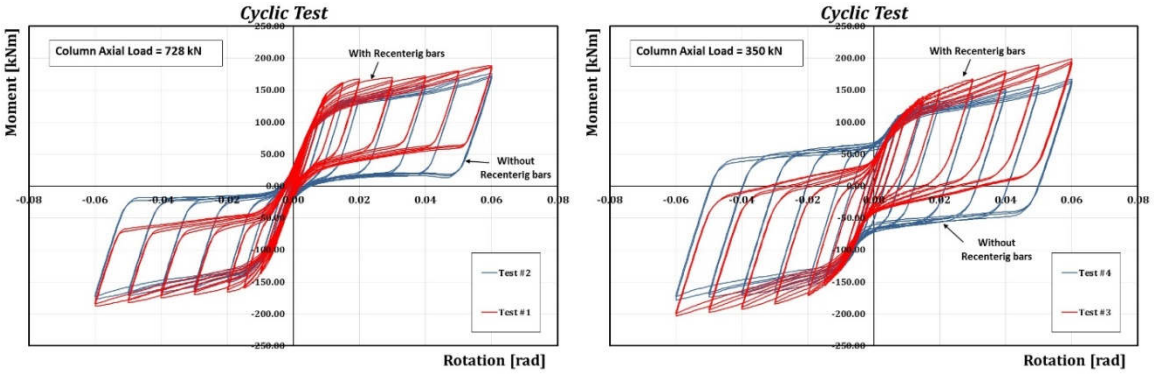

(a) Column Axial Load = 728 kN (b) Column Axial Load = 365 kN

Fig. 6. Moment-Rotation hysteretic curves of tested specimens

Aiming to verify the ability of the proposed column base connection to dissipate energy and to re-center, pseudo-dynamic tests (PsD) have been performed at the Laboratory of Materials and Structures of the University of Salerno. This testing method combines an on-line computer simulation of the dynamic problem (accounting for damping and inertial effects) with experimental data regarding restoring forces and corresponding displacements due to quasi-static application of loads, to provide realistic dynamic response histories even in case of non-linear behavior of severely damaged structures [66]. Its main advantage is that it adopts essentially the same equipment of a conventional quasi-static test, in which prescribed load or displacement histories are imposed on the specimen by means of servo-hydraulic actuators (Fig. 4). The structure to test has been idealized as a discrete-parameter system consisting of one degree of freedom, controlled by the actuator.

458 The classical equation of motion is solved by means of a direct step-by-step integration
459 scheme in which the mass and the viscous damping properties of the structures are modelled
460 analytically while the displacements, and consequently the restoring forces developed by the
461 structure, are measured with the external transducers positioned on a reference frame.
462 In the experimental test the MTS hydraulic actuator was used to apply the displacement
463 history to a system with a fictitious mass equal to 74t. The test was carried out neglecting any
464 additional viscous damping and applying a loading velocity equal to 0.1 mm/s.
465 In order to perform the tests, the Kobe (Japan, 1995) (record of the 16.1.1995, N-S direction)
466 and Spitak (Armenia, 1988) (record of the 12.7.1988, N-S direction)earthquake records were
467 selected as ground motions. Record scale factors equal to 1.4 (PGA=0,35 g) for the Kobe
468 earthquake and equal to 1 (PGA=0.199 g) for the Spitak earthquake, were considered. The
469 selection of few earthquake records for a limited number of pseudo-dynamic tests is always,
470 under many point of views, arbitrary and cannot be representative of all the possible real
471 cases. In this activity, these two specific records were selected to compare earthquakes with
472 different features. In fact, as it can be noticed also from the response of the specimens, while
473 Kobe is a seismic event inducing a high number of large amplitude cycles, Spitak is
474 characterized mainly by two large reversal and many low amplitude cycles. The scale factor of
475 the seismic events was selected in order to achieve in the connection, approximately, a
476 rotation of 40 mrad.
477 In Fig.7 the moment-rotation plots of the pseudo-dynamic tests are reported. These pictures
478 confirm the improved performance of the proposed column base connections in terms of
479 reduction of the residual rotations (Table 1). Also in this case, the comparison between the
480 moment-rotation curve of the column base connection with and without the re-centering
481 threaded bars (Fig. 8a) evidences the improvement obtained with the adoption of re-
482 centering bars.

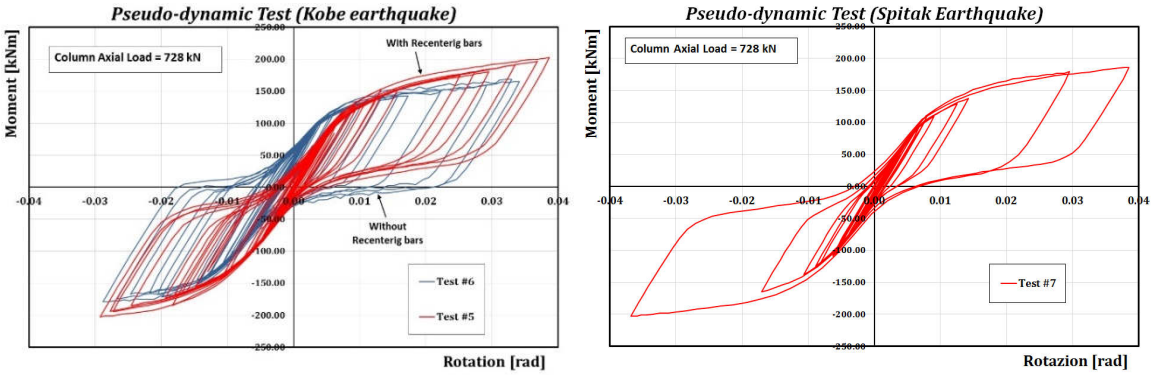

(a) Kobe Earthquake (b) Spitak Earthquake

Fig. 7. Moment-Rotation curves of specimens submitted to pseudodynamic tests

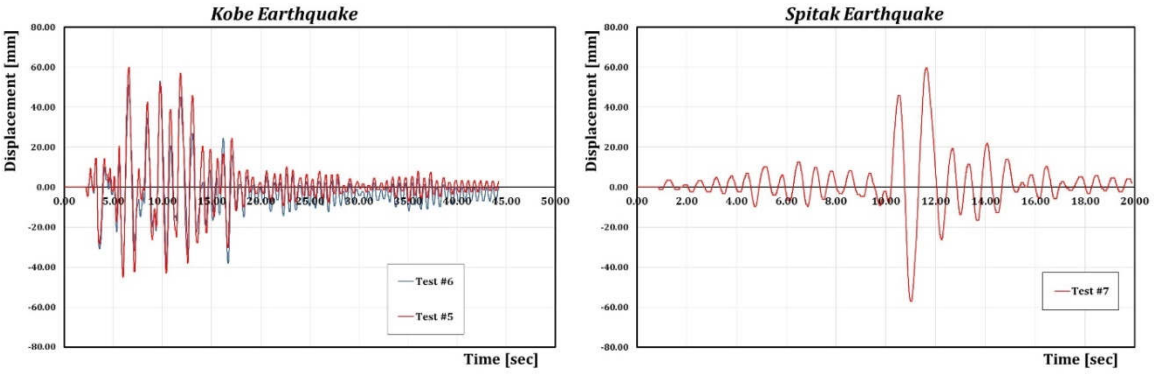

(a) Kobe Earthquake (b) Spitak Earthquake

Fig. 8. Displacement Time-history of specimens submitted to pseudodynamic tests

This effect is also evidenced by the reduction of the residual displacement after the simulated earthquake (Table 1). In Fig.8 the time-history of the displacements at the top of the column are shown for the three pseudo-dynamic tests. It can be observed that the column with the proposed base connection with re-centering bars is characterized by residual displacement after the earthquake always lower than 5 mrad [65].

5. SIMULATIONS OF MRFs

In order to assess the effect of the adoption of the proposed re-centering column base connections over a structure, a preliminary time-history analysis of a MRF has been carried out. The case study structure regards a four bays–six storeys scheme designed according to the Theory of plastic mechanism control [67]. This methodology allows to select the column size applying the upper bound theorem and the concept of mechanism equilibrium curve ensuring the development of a failure mechanism of global type. The achievement of a failure mechanism of global type appears very important in view of the application of a damage

avoidance strategy adopting friction beam-column and self-centering column base connections, as suggested.

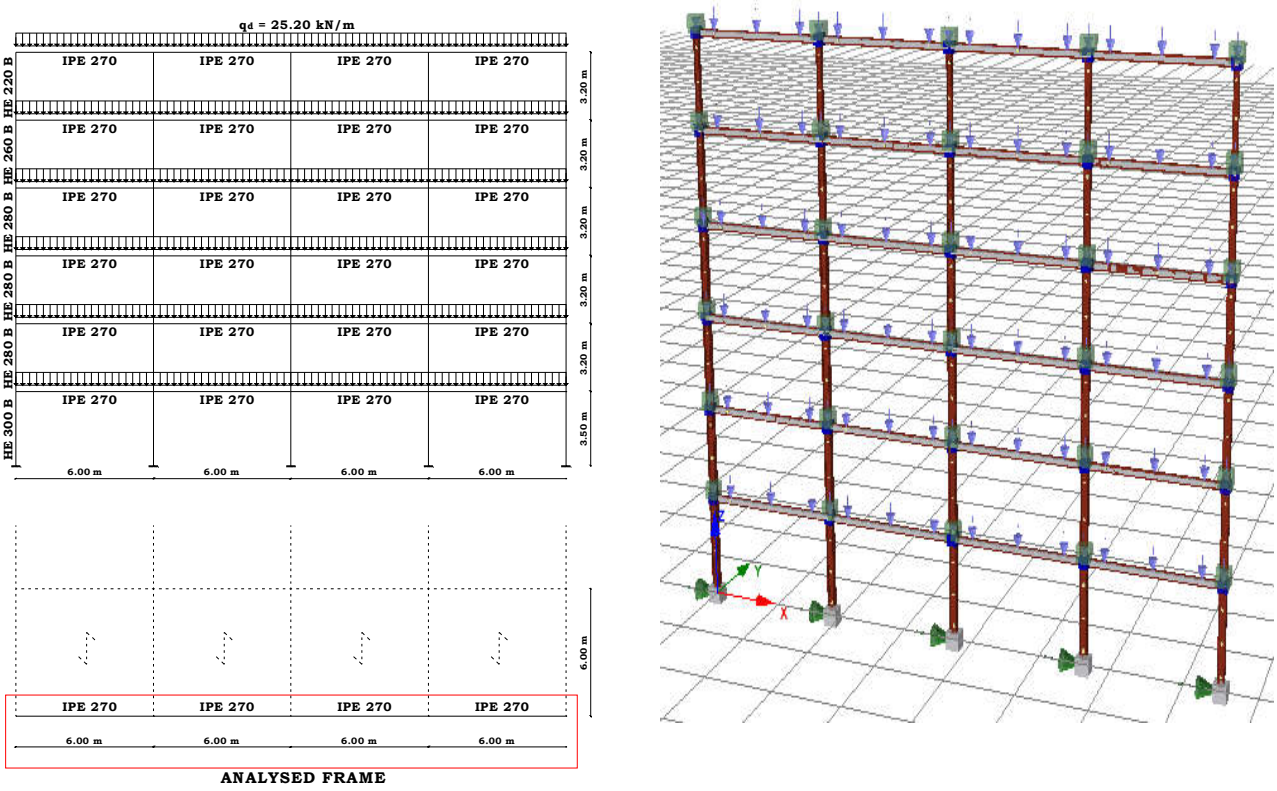

a) b)

Fig. 9. a) Case-study frame. b) Scheme and Seismostruct model

The considered layout has inter-storey heights equal to *3200 mm* except for the first level whose height is equal to *3500 mm,* while the bays have all a span of *6000 mm.* Regarding the loads, a uniform dead load $g_k = 4\ kN/m^2$ and a uniform live load $q_k = 2\ kN/m^2$ (value given by the code for residential buildings) have been considered. Since the analyzed frame is the perimeter frame of the building and the assumed transversal bay span L_t is equal to *6000 mm,* a uniform dead load $G_k = g_k \cdot \frac{L_t}{2} = 12.00\ kN/m$ and a uniform live load $Q_k = q_k \cdot \frac{L_t}{2} = 6\ kN/m$ have been considered, so that the design gravity load distribution has been determined, in accordance with EC8, i.e. $q_v = 1.35G_k + 1.5Q_k = 25.20\ kN/m$. With reference to the seismic combination the load is determined as $q_E = G_k + \psi_2 Q_k + E_d$ (where ψ_2 is the coefficient for the quasi-permanent value of the variable actions, equal to 0.3 for residential buildings) and, as a consequence, the applied reduced gravity load is $q_E = 12 + 0.3 \cdot 6 = 13.8\ kN/m$.

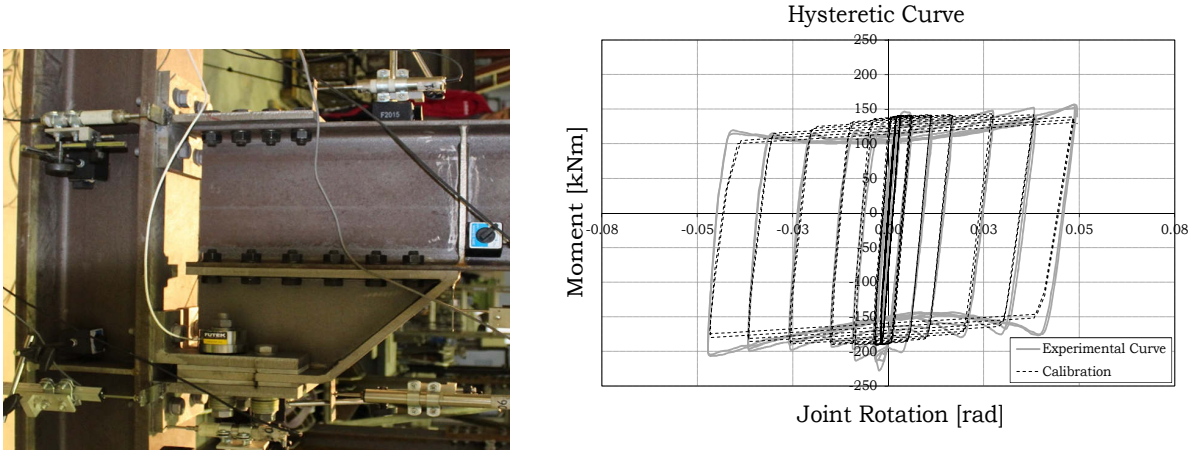

a) b)

520 Fig. 10. a) Beam-to-column connection with friction dampers; b) hysteretic response and
521 calibrated model
522
523 In the dynamic analyses, the seismic masses have been evaluated starting from the uniform
524 distributed loads. The beam has been preliminary sized considering the gravity load
525 combination (and afterwards checked also under seismic loading conditions), leading to the
526 adoption of IPE270 profiles made of S275 steel. The column sections have been selected in
527 order to ensure a failure mechanism of global type, varying the shape at every storey from a
528 maximum of HEB 300 to a minimum of HEB 220 at the top level of the building. The design
529 has been carried out considering a high seismicity region (PGA=0.35 g), soil type C, a seismic
530 response factor equal to 2.5, and a behavior factor equal to 6.

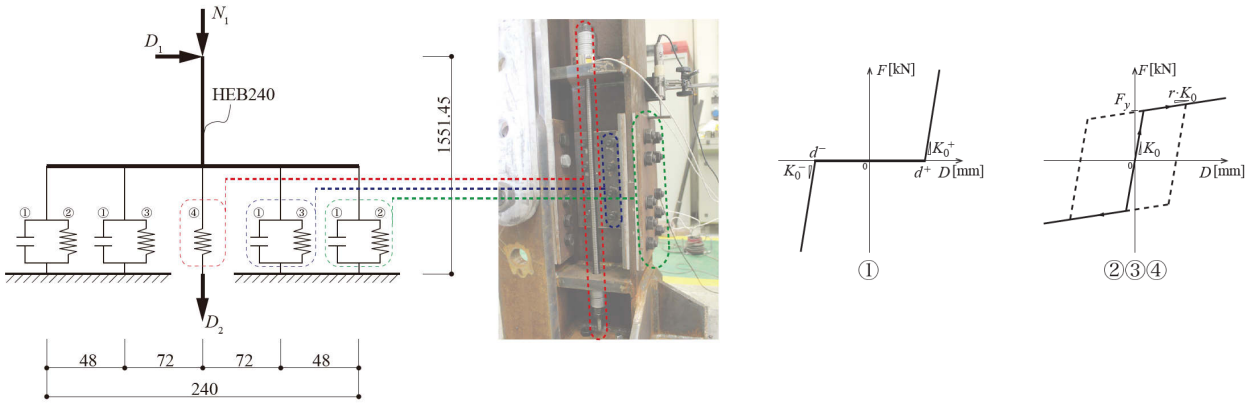

a) Mechanical model of the column base joint b) F-d laws of the adopted springs

531 Fig. 11. Column base joint modelling implemented in Seismostruct [68]

To assess the influence of the proposed connection over the global response, a first comparison has been performed, modelling the frame with the software for dynamic analysis Seismostruct [68] and analyzing the same MRF two times: once assuming a fixed base and, another time, introducing a set of springs able to accurately reproduce the typical behavior of the proposed self-centering connection. In both cases, the assumed beam-to-column connections are the bolted joints with friction dampers already tested in the European research project FREEDAM, whose response is described in [28] (Fig. 9). The hysteretic behavior of the two connection typologies (column base and beam-to-column joint) has been modelled by means of zero-length hysteretic links whose mathematical parameters have been properly calibrated by fitting the experimental moment-rotation response. In case of the beam-to-column joint, a rotational spring has been used to model the connection, defining the parameters by means of the optimization procedure developed in [69]. In this case, to model the hysteresis, the phenomenological model of Sivaselvan and co-authors [70] (commonly called in the software Seismostruct "smooth") has been adopted.

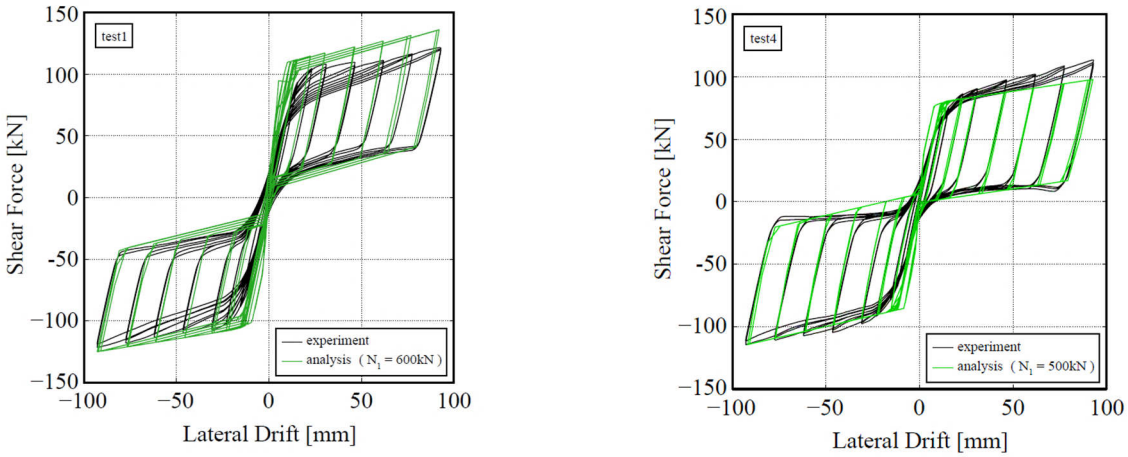

a) N=600 kN b) N=500 kN

Fig. 12. Comparisons between experiments and numerical model for different values of the axial load

Conversely, to model the re-centering column base connections a complete mechanical model based on the assembly of a set of springs able to reproduce the response of the tests previously reported, has been calibrated and verified. This model has been calibrated in order to grasp the effect of interaction between axial load and bending moment over the response of

the connection. The model is composed by four bilinear springs in parallel with gap elements able to simulate the uni-lateral hysteretic response of the friction dampers, plus a central bilinear spring used to model the initial pre-stress of the re-centering bar and the hysteretic response of the bar itself (Fig.11). The yielding force of the springs modelling the friction dampers is determined through Eqs.11 and 15, while the initial stiffness and the slope of the hardening branch has been calibrated on the experimental data, finding the optimized values of K_0=45 kN/mm and r=0.01. Conversely, the stiffness of the spring modelling the re-centering bars has been calculated as previously reported, namely K_{bar+ds}=44.28 kN/mm. The yielding force and the post-elastic stiffness of the recentering bar have been calibrated starting from the experimental data, defining F_y=250 kN and r=0.01. With the selected parameters, the application of the mechanical model to some test results is delivered in Fig.12.

In order to include in the structural model of the MRF the hysteretic behavior of the re-centering connections, the parameters calibrated on the experimental tests have been extended to model the particular configuration employed in the reference building which, in the specific case, represents the connection of an HEB 300 column. In any case, while some model parameters are numerically calibrated by curve fitting, the slip resistance of the friction dampers and the pre-stress of the threaded bars have been re-calculated according to the design procedure previously described in order to achieve the full self-centering capacity of the column base connection.

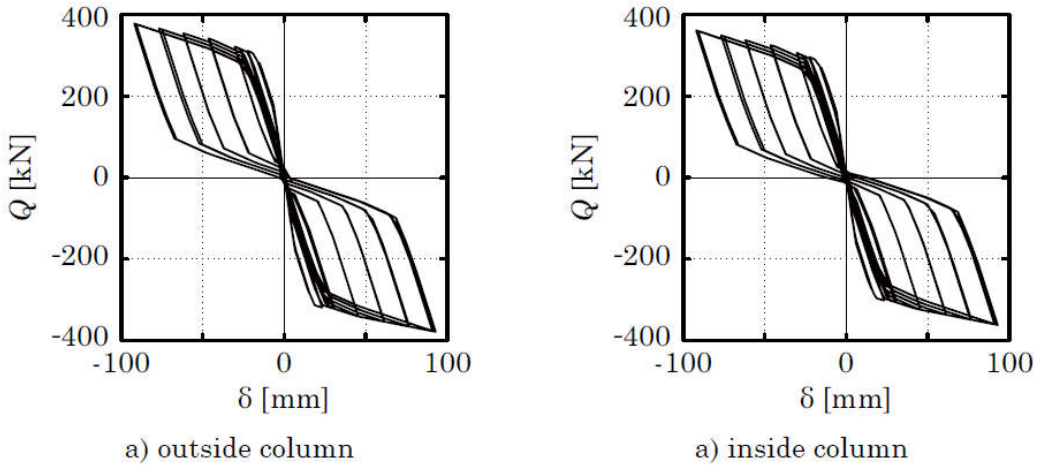

Fig. 13. Behavior of the designed base-plate connections for the case-study frame (Q=Force, δ=displacement), evaluated on a shear length equal to 1.55 m

The results of the design are summarized in Table 2 and Fig.13, for the external and internal columns of the reference MRF. These two typologies need different design values of the pre-

loading applied to the bolts and to the re-centering bars, because they are initially loaded with different values of the axial force (250 kN for the external column, 500 kN for the internal).

Table 2. Model parameters for the re-centering connection (notation explained in Fig.11b)

			External column	Internal column
①	d^+	mm	1000	
	K_0^+	kN/mm	1.0×10^{12}	
	d^-	mm	0.0	
	K_0^-	kN/mm	1.0×10^{6}	
②	K_0	kN/mm	450.0	
	Fy	kN	546.02	549.49
	r		0.01	
③	K_0	kN/mm	450.0	
	Fy	kN	254.44	240.55
	r		0.01	
④	K_0	kN/mm	322.66	
	Fy	kN	1830	1400
	r		0.50	
D		mm	5.67	4.33
N_{act}		kN	250	500

With the calibrated parameters, a time-history analysis of the MRF has been performed, considering the first accelerogram of a set of eight natural records selected to match the EC8 reference elastic pseudo-acceleration spectrum (Fig.14). The fundamental natural period of the structure has been assessed through a modal analysis determining a value of 1.6 seconds. The two structures (fixed bases and self-centering connections) have the same period as the proposed connection, due to the high initial stiffness, is nominally rigid. A damping ratio of the 5% was considered.

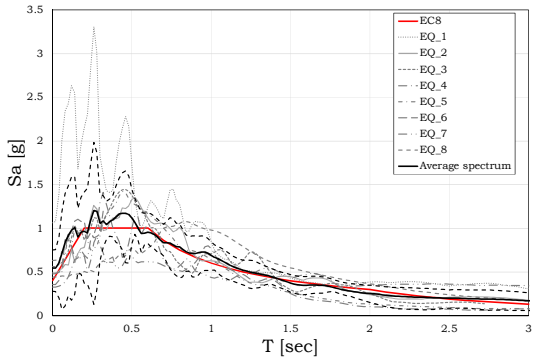

ID	*Earthquake name*	*Date*	*Station name*	*Sation Country*	*Magnitude*	*Fault mechanism*	*PGA [g]*
EQ_1	Alkion	24.02.1981	Xylokastro-O.T.E.	Greece	6.6	Normal	1.066
EQ_2	Montenegro	24.05.1979	Bar-Skupstina Opstine	Montenegro	6.2	Reverse	0.492
EQ_3	Izmit	13.09.1999	Usgs Golden Station Kor	Turkey	5.8	Strike-Slip	0.375
EQ_4	Aigion	15.06.1995	Aigio-OTE	Greece	6.5	Normal	0.313
EQ_5	Umbria-Marche	26.09.1997	Castelnuovo-Assisi	Italy	6.0	Normal	0.369
EQ_6	Izmit	17.08.1999	Istanbul-Zeytinburnu	Turkey	7.4	Strike-Slip	0.480
EQ_7	Olfus	29.05.2008	Ljosafoss-Hydroelectric Power	Iceland	6.3	Strike-Slip	0.315
EQ_8	Olfus	29.05.2008	Selfoss-City Hall	Iceland	6.3	Strike-Slip	0.309

Fig. 14. Time-history response – top storey displacement (red: with re-centering, black: without re-centering)

The results given in Fig.15 highlight the enhanced response showing that with the proposed column base joints it is possible to obtain a significant improvement in terms of residual drifts. In fact, while with traditional full-strength column base connections the residual sway displacement at the top of the building is equal to 350 mm (corresponding to 18 mrad of average inclination of the column), with the employment of the proposed connections, it reduces of about the 85%, achieving a residual top displacement at the end of the simulated seismic event of 60 mm, corresponding to an average inclination of the building of about 3 mrad. This points out that, while with a traditional solution, the actual reparability of the building would be compromised (18 mrad > 5 mrad), with the proposed self-centering connections the residual drift reduces significantly falling within the prescribed limits [65].

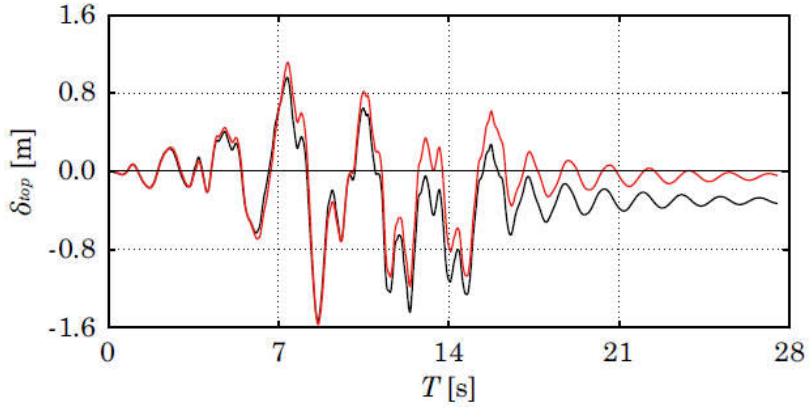

Fig. 15. Time-history response – top storey displacement (red: with self-centering column bases, black: without re-centering)

6. CONCLUSIONS

Aiming to obtain structures undergoing minimal damage able to return also to the original configuration, in this paper, a new type of column base joint equipped with friction dampers and re-centering threaded bars has been suggested. After presenting the conceptual design of the connection, the results of tests and numerical simulations have been reported. The tests carried out on the proposed connection under cyclic and pseudo-dynamic loading conditions have evidenced that, according to the design assumptions, the threaded bars, if properly pre-stressed, are able to work as elastic springs restoring the connection to the initial configuration. On the other hand, the numerical simulations of a case-study MRF have evidenced that, compared to structures with classical full-strength base plate joints, structures with self-centering column bases can self-center returning to the initial

621 configuration. These first analytical results seem promising and suggest extending the work to
622 other configurations in order to provide a wider validation of the system.
623
624 **5. ACKNOWLEDGEMENTS**

625 The research activity herein presented has been supported by the European Community by
626 research grant RFSR-CT-2015-00022. The support of the European Commission within RFCS
627 Research & Innovation is gratefully acknowledged.

628 **REFERENCES**

629 [1] EUROCODE 0. Basis of structural design. CEN, 2010.
630 [2] EUROCODE 1. Action on structures – Part 1-1: General actions – Densities, self-weight,
631 imposed loads for buildings. CEN, 2002.
632 [3] EUROCODE 8. Design of structures for earthquake – Part 1: General rules, seismic actions
633 and rules for buildings. CEN, 2003.
634 [4] Latour M, Rizzano G. (2013). Full Strength Design of Column Base Connections accounting
635 for Random Material Variability. Engineering Structures.48:458-471.
636 [5] Latour M, Rizzano G., 2013. A theoretical model for predicting the rotational capacity of
637 steel base joints. Journal of Constructional Steel Research, 91, pp.89.99
638 [6] D'Aniello M., Tartaglia R., Costanzo S., Landolfo R. (2017). Seismic design of extended
639 stiffened end-plate joints in the framework of Eurocodes. Journal of Constructional Steel
640 Research, Volume 128, January 2017, Pages 512–527
641 [7] Tartaglia R., D'Aniello M., Rassati G.A., Swanson J.A., Landolfo R. (2018). Full strength
642 extended stiffened end-plate joints: AISC vs recent European design criteria. Engineering
643 Structures, Volume 159, 15 March 2018, Pages 155–171.
644 [8] Hart (1994). Typical Costs for Seismic Rehabilitation of Existing Buildings, Volume I:
645 Summary (FEMA 156), prepared by the Hart Consultant Group for the Federal
646 Management Agency, Washington, D.C.
647 [9] Hart (1995). Typical Costs for Seismic Rehabilitation of Existing Buildings, Volume II:
648 Supporting Documentation (FEMA 157), prepared by the Hart Consultant Group for the
649 Federal Management Agency, Washington, D.C.

650 [10] Hwang, H.M., Xu, M., and Huo, J.-R. (1994), Estimation of Seismic Damage and Repair Cost
651 of the University of Memphis Buildings, Memphis, Tennessee.
652 [11] Dimopoulos, A. I., Tzimas, A. S., Karavasilis, T. L., and Vamvatsikos, D. (2016) Probabilistic
653 economic seismic loss estimation in steel buildings using post-tensioned moment-
654 resisting frames and viscous dampers. Earthquake Engng Struct. Dyn., 45: 1725–1741.
655 doi: 10.1002/eqe.2722.
656 [12] Latour M., Piluso V., Rizzano G. "Free from damage beam-to-column joints: Testing and
657 design of DST connections with friction pads." Engineering Structures, 2015.
658 [13] MacRae G.A., Clifton G.C., Mackinven H., Mago N., Butterworth J., Pampanin S. "The sliding
659 hinge joint moment connection." Bulletin of New Zealand society for earthquake
660 engineering, vol.43, n.3, September 2010.
661 [14] Ramhormozian, S., Clifton, G. C. (2016). "Recent Developments on the Sliding Hinge Joint".
662 Proceedings of the NZSEE Conference.
663 [15] Freddi, F., Dimopoulos, C.A., Karavasilis, T.L. Rocking damage-free steel column base with
664 friction devices: design procedure and numerical evaluation (2017) Earthquake
665 Engineering and Structural Dynamics, 46 (14), pp. 2281-2300.
666 [16] Grigorian CE, Yang TS, Popov EP. 1993 "Slotted bolted connection energy dissipators".
667 Earthquake Spectra. Vol.9, No.3, pp.491-504.
668 [17] Clifton GC, Butterwoth JW, (2000). Moment-resisting steel framed seismic-resisting
669 systems with semi-rigid connections 12th WCEE, Auckland, New Zealand.
670 [18] Clifton GC, Zaki R, Butterwoth JW, (2004). Damage-resistance steel framed seismic-
671 resisting systems. 13th WCEE, Vancouver, Canada.
672 [19] Golondrino JC, MacRae G, Chase J, Rodgers G., Clifton GC. Velocity effects on the behavior
673 of asymmetrical friction connections (AFC). 8th STESSA Conference, Shanghai, China, July
674 1-3, 2015
675 [20] Khoo, H., Clifton, C. Butterworth, J. MacRae, G. Ferguson, G. 2012. "Influence of steel shim
676 hardness on the sliding hinge joint performance". Journal f Constructional Steel Research,
677 72, 119-129.
678 [21] Ramhormozian S., Clifton G.C., MacRae G.A. "The Asymmetric Friction Connection with
679 Belleville springs in the Sliding Hinge Joint" NZSEE Conference, 2014.

680 [22] Ramhormozian S., Clifton G.C., Nguyen H., Cowle K. “Determination of the required part-
681 turn of the nut with respect to the number of free threads under the loaded face of the nut
682 in fully tensioned high strength friction grip property class 8.8 bolts.” Steel Innovations
683 Conference, 2015.
684 [23] Yokoyama S, Oki T. “Connecting Structure of beam and column and building having it
685 structure” JP2000328650 (A) — 2000-11-28.
686 [24] Inoue K, Higashihata Y, Takahashi K, Ishii O “Anti-seismic damper using bolt drive”
687 JPH0366877 (A) — 1991-03-22.
688 [25] Latour M, Piluso V, Rizzano G. (2011). Experimental analysis of innovative dissipative
689 bolted double split tee beam-to-column connections. Steel Construction. June;4(2):53-64.
690 [26] Ferrante Cavallaro G., Francavilla A., Latour M., Piluso V., Rizzano G. Experimental
691 behaviour of innovative thermal spray coating materials for FREEDAM joints.
692 Composities Part B Engineering, September 2016
693 [27] Latour, M., Piluso, V. and Rizzano, G. (2014). "Experimental Analysis on Friction Materials
694 for Supplemental Damping Devices". Construction and Building Materials, Vol. 65,
695 pp.159–176.
696 [28] M. Latour, M. D’Aniello, M. Zimbru, G. Rizzano, V. Piluso, R. Landolfo, Removable friction
697 dampers for low-damage steel beam-to-column joints, Soil Dynamics and Earthquake
698 Engineering, Volume 115, 2018, Pages 66-81.
699 [29] Heistermann C. “Behaviour of pretensioned bolts in friction connections.” Licentiate
700 thesis. Lulea, June 2011.
701 [30] EN 1090-2. Execution of steel structures and aluminium structures: technical
702 requirements for steel structures. CEN, 2008.
703 [31] EN 14399-1. High-strength structural bolting assemblies for preloading - Part 1: General
704 requirements. CEN, 2015.
705 [32] EN ISO 898-1. Mechanical properties of fasteners made of carbon steel and alloy steel -
706 Part 1: Bolts, screws and studs with specified property classes - Coarse thread and fine
707 pitch thread.
708 [33] EN 15048-1. Non – preloaded structural bolting assemblies. General requirements. CEN,
709 2007.

710 [34] Berenbak J. Evaluation tightening preloaded bolt assemblies according to EN 1090-2.
711 CEN/TC 135 WG2, June 2012.
712 [35] Iyama J, Seo CY, Ricles JM and Sause R. (2009), “Self-centering MRFs with Bottom Flange
713 Friction Devices under Earthquake Loading,” Journal of Constructional Steel Research, 65
714 (2) :314–325.
715 [36] MacRae, G. A. , Urmson, C. R. , Walpole, W. R., Moss, P. , Hyde K. and Clifton, C. (2009)
716 "Axial Shortening of Steel Columns in Buildings Subjected to Earthquakes," Bulletin
717 NZSEE, vol. 42, p. 275.
718 [37] Borzouie, J. , MacRae, G.A., Chase, J.G., Rodgers, G.W., Clifton, G.C. (2015). “Column base
719 weak axis aligned asymmetric friction connection cyclic performance”, 8th International
720 Conference on Behavior of Steel Structures in Seismic Areas Shanghai, China, July 1-3.
721 [38] Silva L., (2016). “Design of a “Free From Damage” Base Column Connection for Seismic
722 Actions”, Msc Thesis in Civil Engineering, FCTUC – Universidade de Coimbra, July 2016.
723 Supervisors: Aldina Santiago, Luis Simões
724 [39] Khoo, H-H., Clifton, C., Butterworth, J., and Macrae, G. (2013). “Experimental Study of Full-
725 Scale Self-Centering Sliding Hinge Joint Connections with Friction Ring Springs”. Journal
726 of Earthquake Engineering, Vol. 17, pp. 972-997.
727 [40] Zhang, A-I., Zhang, Y-X, Li, R., Wang, Z-Y. (2016). “Cyclic behaviour of a prefabricated self-
728 centering beam–column connection with a bolted web friction device”. Engineering
729 Structures, Vol. 111.
730 [41] Chi, H., & Liu, J. (2012). Seismic behavior of post-tensioned column base for steel self-
731 centering moment resisting frame. Journal of Constructional Steel Research, 78, 117-130.
732 [42] Baiguera, M., Vasdravellis, G., Karavasilis, T.L. Dual seismic-resistant steel frame with
733 high post-yield stiffness energy-dissipative braces for residual drift reduction (2016).
734 Journal of Constructional Steel Research, 122, pp. 198-212.
735 [43] Dimopoulos, A.I., Karavasilis, T.L., Vasdravellis, G., Uy, B. Seismic design, modelling and
736 assessment of self-centering steel frames using post-tensioned connections with web
737 hourglass shape pins (2013) Bulletin of Earthquake Engineering, 11 (5), pp. 1797-1816.
738 [44] Vasdravellis, G., Karavasilis, T.L., Uy, B. Finite element models and cyclic behavior of self-
739 centering steel post-tensioned connections with web hourglass pins (2013) Engineering
740 Structures, 52, pp. 1-16.

741 [45] T.T. Soong, B.F. Spencer, Supplemental energy dissipation: state-of-the-art and state-of-
742 the-practice, Engineering Structures, Volume 24, Issue 3, 2002, Pages 243-259
743 [46] Chen L., Jinbao, J., Huage, J., Honguy, Z. "Hydraulic friction damper with adjustable friction
744 force" CN201611113822 20161207
745 [47] A Semi-Active Electromagnetic Friction Damper for Response Control of Structures A. K.
746 Agrawal ; and J. N. Yang Advanced Technology in Structural Engineering . 2000
747 [48] Latour M, Piluso V, Rizzano G. (2014). Experimental Analysis of Friction Materials for
748 supplemental damping devices. Construction and Building Materials.
749 [49] W. Loo, W., Quenneville, P. and Chouw N. (2015). "Steel friction connectors – the dangers
750 of excess smoothing", Proceedings of the NZSEE Conference.
751 [50] Pall, A. & Marsh, C., 1981. Response of Friction Damped Braced Frames. Journal of the
752 Structural Division, 108(6), pp.1313-23.
753 [51] Tremblay, R. & Stiemer, S., 1993. Energy Dissipation through Friction Bolted Connections
754 in Concentrically Braced Steel Frames. ATC 17-1 Seminar on Seismic Isolation, 2, pp.557-
755 68.
756 [52] Mualla, I. & Belev, B., 2002. Seismic Response of Steel Frames Equipped with a New
757 Friction Damper Device Under Earthquake Excitation. Engineering Structures, 24(3),
758 pp.365-71.
759 [53] Wei Y. Loo, Pierre Quenneville, Nawawi Chouw, A new type of symmetric slip-friction
760 connector, Journal of Constructional Steel Research, Volume 94, 2014, Pages 11-22
761 [54] G.W. Rodgers, J.G. Chase, R. Causse, J. Chanchi, G.A. MacRae, Performance and degradation
762 of sliding steel friction connections: Impact of velocity, corrosion coating and shim ma-
763 terial, Engineering Structures, Volume 141, 15 June 2017, Pages 292-302
764 [55] Paolo Negro, Marco Lamperti Tornaghi, Seismic response of precast structures with
765 vertical cladding panels: The SAFECLADDING experimental campaign, Engineering
766 Structures, Volume 132, 1 February 2017, Pages 205-228
767 [56] Bruno Dal Lago, Fabio Biondini, Giandomenico Toniolo, Friction-based dissipative
768 devices for precast concrete panels, Engineering Structures, Volume 147, 15 September
769 2017, Pages 356-371

[57] Gledhill, S.M., Sidwell, G.K., Bell, D.K., The Damage Avoidance Design of tall steel frame buildings - Fairlie Terrace Student Accommodation Project", Victoria University of Wellington

[58] MacRae, G. A. , Urmson, C. R. , Walpole, W. R., Moss, P. , Hyde K. and Clifton, C. (2009) "Axial Shortening of Steel Columns in Buildings Subjected to Earthquakes," Bulletin NZSEE, vol. 42, p. 275.

[59] Borzouie, J. , MacRae, G.A., Chase, J.G., Rodgers, G.W., Clifton, G.C. (2015). "Column base weak axis aligned asymmetric friction connection cyclic performance", 8th International Conference on Behavior of Steel Structures in Seismic Areas Shanghai, China, July 1-3.

[60] Elkady, Lignos Full-Scale Testing of Deep Wide-Flange Steel Columns under Multiaxis Cyclic Loading: Loading Sequence, Boundary Effects, and Lateral Stability Bracing Force Demands Ahmed

[61] ANSI/AISC 341-16 (2016), "Seismic Provisions for Structural Steel Buildings". Chicago, Illinois, USA.

[62] Ferrante Cavallaro G., Francavilla A., Latour M., Piluso V, Rizzano G (2018). "Cyclic Behaviour of Friction materials for low yielding connections". November 2018Soil Dynamics and Earthquake Engineering 114:404-423

[63] Montuori R, Nastri E, Piluso V, Streppone S, D'Aniello M, Zimbru M, Landolfo R (2018). "Comparison Between Different Design Strategies For Freedam Frames: Push-Overs and Ida Analyses". The Open Civil Engineering Journal, Vol.12, 140-153

[64] Wald F, Sokol Z, Steenhuis M, Jaspart JP, "Component method for steel column bases". HERON journal. 53-12

[65] Mc Cormik, J, Aburano, H, Ikenaga, M, Nakashima, M, (2008) "Permissible residual deformation levels for building structures considering both safety and huma elements". 14th WCEE, Beijing, China.

[66] P. Shing, P. and S. Mahin, (1984) "Pseudodynamic test method for seismic performance evaluation: Theory and implementation," Earthquake Engineering Research Center UCB/EERC-8'1/01, University of California, Berkeley

[67] Longo A., Nastri E., Piluso V. (2015) "Theory of Plastic Mechanism Control: State of the art." The Open Construction and Building Technology Journal 8(1):262-278

800 [68] Seismosoft, “SeismoStruct - A computer program for static and dynamic nonlinear
801 analysis of framed structures". Available from URL: www.seismosoft.com
802 [69] Chisari, C., Francavilla, A.B., Latour, M., Piluso, V., Rizzano, G., Amadio, C. (2017) Critical
803 issues in parameter calibration of cyclic models for steel members. Engineering
804 Structures, 132, pp. 123-138.
805 [70] Sivaselvan MV, Reinhorn AM. (2000) Hysteretic models for deteriorating inelastic
806 structures. J Eng Mech 2000;126(6):633–40.
807 [71] Tenchini A., D’Aniello M., Rebelo C., Landolfo R., da Silva L.S., Lima L. (2014). Seismic
808 performance of dual-steel moment resisting frames. Journal of Constructional Steel
809 Research, Volume 101, October 2014, pp. 437-454.
810 [72] Cassiano D., D’Aniello M., Rebelo C., Landolfo R., da Silva L. (2016). Influence of seismic
811 design rules on the robustness of steel moment resisting frames. Steel and Composite
812 Structures, An International Journal, Volume 21, Number 3, , pp. 479-500, June30 2016.
813